

State-of-the-art Potential Clamp Device for Myelinated Nerve Fibres Using a New Versatile Input Probe

K H BOHUSLAVIZKI, A KNEIP and E KOPPENHOFER

*Institute of Physiology, University of Kiel,
Olshausenstr 40, 24098 Kiel, Germany*

Abstract. A potential clamp device for myelinated axons is presented which, for the first time, systematically optimizes all the methodological parameters that limit the reliability of ionic current measurements. A crucial step toward this end consisted in the development of a new input probe with broad-band, extremely low-capacitance characteristics. In combination with a simple-to-use compensation criterion for optimum positive feedback, based on plausible assumptions, and with additional technological improvements, it enables the measurement of ionic currents with a reliability never previously achieved. The consequences with respect to evaluation of several earlier findings are discussed.

Key words: Node of Ranvier — Potential clamp device — Reliability of data — Input probe — Floating supply — Bootstrap circuit

Introduction

Since the very beginning of research on electrical excitability, stimulus currents have been applied and the resulting potential changes recorded (Koppenhofer et al 1992). However it was not until rectangular potential pulses were used rather than current pulses, and the membrane currents they produced were evaluated (Marmont 1949, Hodgkin et al 1949), that way was clear to our present understanding of potential-dependent ion channels. With this new technique, called potential clamping, the potential- and time-dependence of the underlying ion permeabilities were soon quantitatively described (Hodgkin and Huxley 1952, Frankenhaeuser and Huxley 1964). This HHF description subsequently gave rise to many models of the mechanism of excitation. The precision of the measurements that is, the reliability of the data on which the models were based – was decisive, for “at best the criterion (of agreement between theory and measurement) must be in agreement within the

Correspondence to Prof Dr med E Koppenhofer, Institute of Physiology, University of Kiel, Olshausenstraße 40, 24098 Kiel, Germany

limits of accuracy of the measuring instruments employed" (Kuhn 1961).

When the potential-clamp technique was extended to myelinated nerve fibres, particular difficulties were encountered in this regard, because their axons are too small to permit intracellular-microelectrode recording of the membrane potential with sufficient long-term stability. Therefore it was necessary to resort to electrical compartmentalization of the axon; a potential-recording negative feedback system was introduced which employed ordinary unpolarizable electrodes, one of which was virtually situated at the inner side of the membrane (Frankenhaeuser 1957). However, potential clamp measurements *per se* require a feedback system; thus the intermeshed two-loop feedback system for Ranvier nodes according to Frankenhaeuser was developed (Dodge and Frankenhaeuser 1958).

There has been no lack of attempts to simplify this technically elaborate measurement procedure. Of the many proposed solutions, the potential clamp system of Nonner (1969) has become the most widely known, because most of the findings related to the mechanism of Ranvier node function in the last 25 years have been obtained with this method.

A number of authors have pointed out the limitations of the Nonner method and all those derived from it (Sommer et al. 1982; Koppenhöfer and Bohuslavizki 1988; Albers et al. 1989). Here we describe a method for the measurement of ionic currents at the node of Ranvier that has been derived from Frankenhaeuser's two-loop method and optimized wherever technically possible.

The Problem

Our efforts were directed toward optimizing the reliability of membrane current records – that is to minimize all parameters that can introduce error into the time course and potential dependence of the current as recorded. To this end, what is needed is: 1) to optimize the quality of control of the measuring system, 2) to linearize the transfer function of the internode serving as a current-measuring impedance, 3) to minimize the influence of the voltage drop at the Schwann-cell structures in the nodal gap, 4) to enable rapid checking of the degree of system optimization achieved in each case during the experiment as well as subsequent adjustment, if required, and 5) to optimize the zero-drift of the measurement system.

Materials and Methods

General

The isolated *Xenopus* fibre to be investigated was positioned along the four pools of a recording chamber in the ordinary way, so that the Ranvier node of interest was in pool A, which was continuously perfused with Ringer solution (Fig. 1). The pools were isolated from one another by Vaseline seals about 100 μm thick (hatched). The cut ends of the

axon were in pools C and E; for further general details see Bohuslavizki et al. (1994).

Because in potential clamp devices the axon is situated in the feedback loops of the electronic system, in order to maximize the time resolution of the current records thick and hence relatively broad-band axons are basically preferable; the dissection technique of Koppenhöfer et al. (1987) provides significantly thicker axons than comparable procedures.

A prerequisite for ionic current measurements with maximal time resolution and precision is that the control of the membrane potential is optimized with respect to precision and speed. In the interest of optimal quality of control (Pressler 1967), therefore, the system must be subdivided into a potential-controlling and a membrane-current-recording loop.

So that the potential-controlling loop can be optimally adapted to different axons, a tunable PI amplifier (A1) is required. Because the input resistance of this amplifier is necessarily high, for the sake of optimal speed of control special steps must be taken to reduce the effective input capacitance, which comprises the input capacitance of the input probe *per se* plus the stray capacitances of the input electrode, its connections, and of pool C of the chamber. Devices with negative capacitance (see, e.g., Neher 1974; Purves 1981; Smith et al. 1985) are fundamentally unsuitable for such control systems, primarily because of inadequate system stability. In the present case, therefore, the lowest input capacitance can be achieved only with an input probe in a bootstrap circuit with floating supply (Mozhayev 1968; Kootsey and Johnson 1973, Schumann 1980). Furthermore, this technique allows effective shielding of the C electrode and pool C in that the pool B, which shields pool C from below and the side, is capacitively driven as well. In this respect the device resembles that of Mozhayeva et al. (1977). With such an input probe, the corner frequency of the transfer function of the internode \overline{DC} is shifted into the region of several 100 kHz, so that the phase reserve of the closed loop is considerably enlarged (cf. Albers et al. 1989, Fig. 4). The result is broad-band compensation of the electrical influence of the Schwann-cell structures in the nodal gap.

The transfer function of the internode \overline{DE} has high-pass characteristics, which have the effect of a low-pass filter on the membrane current records. This can be counteracted by putting an additional, grounded pool between pools A and E (Koppenhöfer and Schumann 1981; Schumann et al. 1983), but it is simpler and equally effective to provide an appropriate switchable low-pass filter in series (Fig. 1, CN) (Kneip 1987).

All the older potential clamp devices for myelinated axons are based on the assumption that the nodal gap is of such low impedance that the A electrode, to a close approximation, is functionally in direct contact with the outside of the membrane. Electron microscopic studies have shown this assumption to be erroneous (Berthold and Rydmark 1983 a,b; R.-G. Sommer, unpublished). Considering this structure as a series resistance, membrane physiologists used to try to minimize the voltage drop that the membrane current induces here by partially blocking the ionic currents, but this method is not very effective, as it certainly does not reduce the delay in membrane potential changes. On the other hand, lack of compensation for the series resistance introduces both amplitude and dynamic distortions in the ionic current measurements, which depend on the membrane conductance, the ionic equilibrium potentials and the command voltages (Ramón et al. 1975). The necessity of full compensation for series resistance errors becomes obvious in experiments that employ the time course of ionic currents to choose between possible models. Finally, questions have been raised about whether or not several reports of experimental observations at variance with the Hodgkin-Huxley description might be

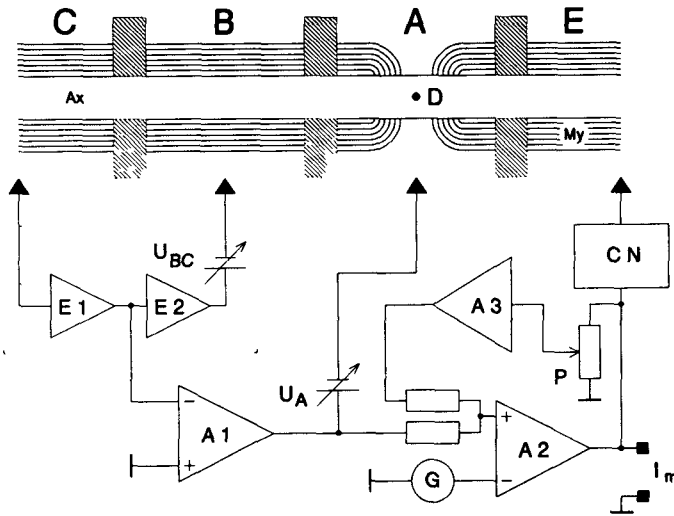


Figure 1. Schematic diagram of the experimental setup. Ax: axon cylinder; My: myelin lamellae of the two internodes of the nerve fibre, cut off at right and left; A,B,C,E: liquid-filled pools; D: point inside the axon cylinder close to the node under investigation; hatched areas: Vaseline partitions; A1,A2: operational amplifiers with adjustable frequency responses (not shown); A3: buffer amplifier; P: adjustment of the electronic positive feedback to compensate the influence of the series resistance; CN: switchable compensation network for linearization of the current-measuring internode in pool E; G: digital stimulator; E1,E2: low-capacitance input probe (for further details see Fig. 2); U_{BC} , U_A : adjustable voltage sources; I_m : output for membrane current records.

caused by uncompensated series resistance (Moore et al. 1984). So far no attempts to position a potential-recording electrode reliably in the periaxonal space at an intact node, between axolemma and the overlying Schwann cell (cf. Bohuslavizki et al. 1994, Fig. 7), have succeeded; thus the only method at present available to render innocuous the voltage drop caused by the nodal-gap structures relies on current-proportional positive feedback (Hodgkin et al. 1952; Koppenhöfer and Schumann 1979; Sigworth 1980). It is based on the assumption that the behaviour of the Schwann-cell structures in the nodal gap is purely ohmic; we have found no grounds for calling this simplification into question.

In our device the current-recording loop consists of the Ranvier node under investigation, the current-measuring internode \overline{DE} , the above-mentioned linearizing low-pass filter CN and the actual clamp amplifier A2, which like A1 has the form of a tunable PI amplifier. The current-proportional positive feedback is mediated by the potentiometer P, the buffer amplifier A3 and a 100-kHz first-order filter (not shown).

Input probe

The input probe described here (Fig. 2) consists of two operational amplifiers E1 and E2 with the amplification +1. Hence the input probe represents an impedance transformer with an overall amplification of +1. The amplifier E2 is powered by a symmetrical supply

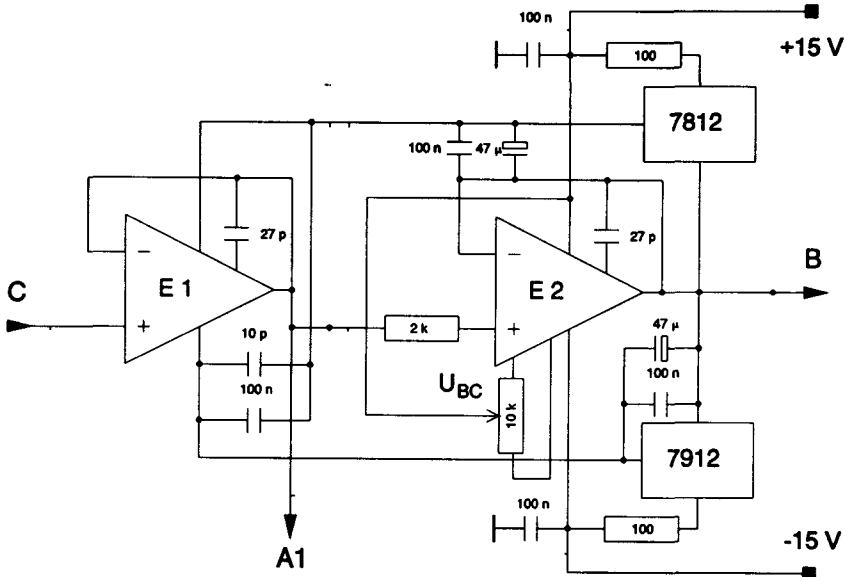


Figure 2. Detailed circuit diagram for the low-capacitance input probe. E1, E2 operational amplifiers (Type 1437, Teledyne Philbrick, Dedham MA), 7812, 7912 conventional voltage regulators, U_{BC} trimmer to compensate the electrode potential between pools B and C. C, B electrode connections in the corresponding pools, A1 connection to amplifier A1. Further details in text.

voltage (± 15 V) and provides the virtual ground for the voltage regulators (7812, 7912). These generate the supply voltage for the amplifier E1, which is constant with respect to the output B. Because the output voltage of E2 corresponds to the input signal of the input probe in the working range of the latter, the supply voltage of E1 is shifted by the same amount as its input signal. Both amplifier inputs, in particular all components connected to the input of E1, are shielded with the associated output. As a result, the dynamic input capacitance of the whole device is made very low. The measured frequency response of the input capacitance of the C input is shown in Fig. 3.

Setting of positive feedback

Because of the above-mentioned electrical inaccessibility of the periaxonal space, all criteria for optimal compensation of the influence of the series resistance are based on more or less plausible assumptions.

Current clamp methods for determining the optimal amount of compensation (Binstock et al. 1975) seem to us to be useless for the node of Ranvier because of the unsuitable signal-to-noise ratio. The so-called sine wave admittance technique, based on the idea of separating the capacitive current from the ionic currents and feeding back only the latter (Moore et al. 1984), we regard as a technically elaborate compromise that is not needed for the myelinated axon. In contrast, the compensation criteria we have thoroughly tested demand no special technical features.

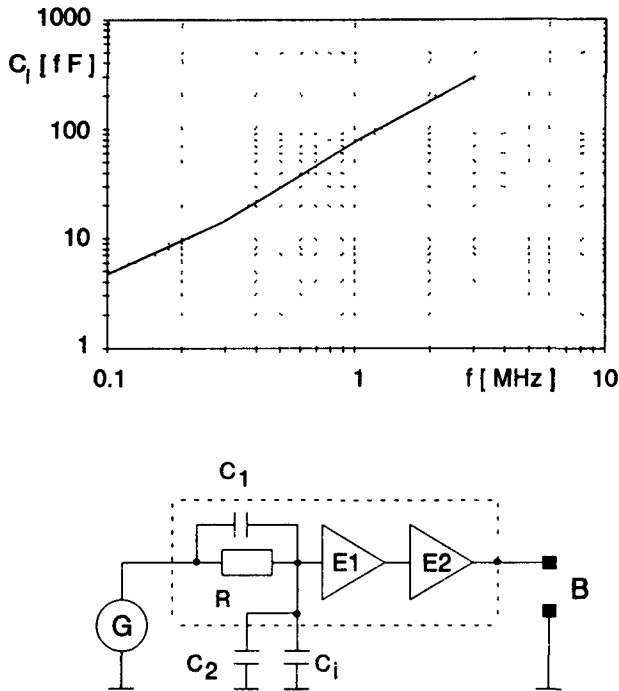


Figure 3. Top: frequency response of the input capacitance C_i of the input probe shown in Fig. 2. Bottom: Test assembly with which the above curve was measured. E1,E2: simplified diagram of the tested input stage; C_i : input capacitance; $R = 150 \text{ M}\Omega$; C_1 : shunt capacitance of R ; $C_2 = 1 \text{ pF}$; G : sine-wave generator; B : output. Procedure: 1. Calculation of C_1 by the transfer function of the test circuit assuming $C_i \ll C_2$. 2. Removal of C_2 . 3. Calculation of C_i by the transfer function of the input probe. Note that thorough shielding (dotted line) is mandatory.

Ramón et al. (1975) carried out calculations to correct the standard data of the squid axon for the influence of series resistance in this preparation and obtained sodium current-voltage curves with a minimum at the membrane potential close to $E = 0$. It was a simple matter to produce such current-voltage curves at the node of Ranvier (with a suitable amount of positive feedback); however, we consider this “ $E = 0$ criterion” inappropriate, because it has since turned out that the necessary measurements of the resting potential (cf. Wiese and Duchâteau 1984) can be seriously faulty in individual cases. Starting from the assumption that under resting conditions the inactivation of the sodium system amounts to about 20%, so that $h_\infty \approx 0.8$, voltages measured in pool A with point D (i.e., ground) as reference were found to lie between -30 and well over $+100$ mV.

This difficulty can be avoided by basing the compensation criterion on the fact that the above-mentioned sodium current-voltage curve, calculated by Ramón et al. (1975), is in addition symmetrical. Such current-voltage curves can also easily be produced with a

suitable amount of positive feedback. It was notable, however, that with this “symmetry criterion” the series resistances calculated from the necessary amounts of positive feedback, 413 k Ω (median; range 224 to 916 k Ω ; $n = 36$), were somewhat larger than with the $E = 0$ criterion (240 k Ω ; 190 to 840 k Ω ; $n = 6$) (Albers et al. 1989; Bethge et al. 1991).

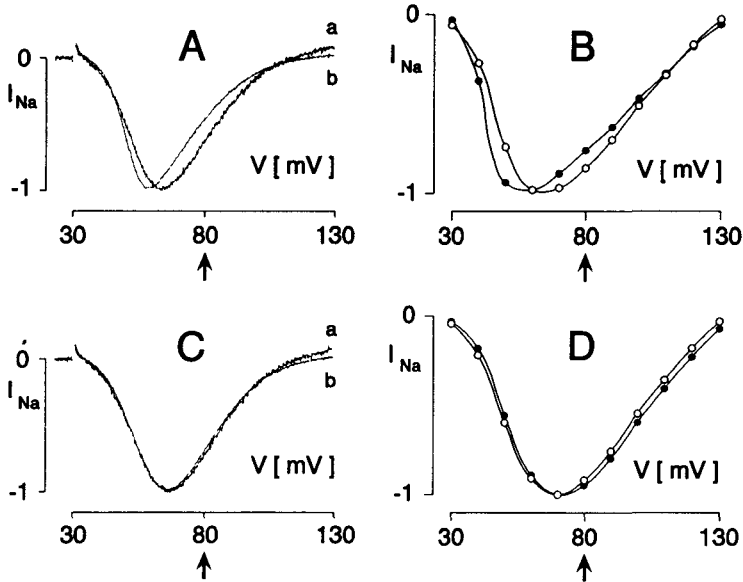


Figure 4. Compensation of the influence of the series resistance. Abscissa: test-pulse amplitude V in mV; ordinate: normalized sodium currents I_{Na} elicited after various prepulses; *A, C*: current-voltage curves obtained with ramp pulses (30 V/s). *B, D*: current-voltage curves for the peak sodium currents, obtained with rectangular pulses, spline interpolation (Wiese and Koppenhöfer 1988); *a*, open symbols: with prepulses having $V = +15$ mV and duration 50 ms; *b*, filled symbols: with prepulses having $V = -40$ mV and duration 50 ms. *A, B*: without compensation. *C, D*: with compensation applying the ramp criterion. Arrows denote zero membrane potential ($E = 0$ mV) assuming that the potential measured in pool A *versus* ground indicates the absolute membrane potential. All data from a single axon.

A disadvantage of both compensation criteria is that they are based on the analogy between unmyelinated and myelinated axons. This can be circumvented by choosing the degree of compensation so that the time course of the recorded sodium currents does not depend on their amplitude – for example, is not affected by the conditioning prepulses applied before the test pulses (Chiu 1980). This criterion, based only on the validity of the HHF description, is very time-consuming when rectangular pulses are used and hence is regarded as obsolete. Therefore we applied ramp pulses, which gave continuous current-voltage curves between $V = 30$ mV and $V = 130$ mV and which were immediately preceded by hyperpolarizing or depolarizing rectangular prepulses of duration sufficient to increase or reduce the sodium currents. The slope of the ramp pulses was adjusted so that the membrane current records showed predominantly sodium currents (Fig. 4 left).

In the absence of compensation the kinetics of the sodium currents elicited after different prepulses and normalized to the same amplitude were, as expected, distinctly different (*A*); the peak sodium currents elicited with rectangular pulses and normalized in this way also gave horizontally shifted current-voltage curves (*B*). Then the degree of compensation was increased with the potentiometer *P* until both the ramp-induced (normalized) sodium currents and the (normalized) sodium current-voltage curves determined with rectangular pulses were independent of the magnitude of the available sodium current (Fig. 4, *C* and *D*). The series resistances found with this compensation criterion had a median value of 127 k Ω (range: 7–610 k Ω ; $n = 57$).

Results

Quality of control

Three simple ways to test the speed and quality of control achieved by the improvements listed above at any time during an experiment are shown in Fig. 5. The transfer function of the controlled member \overline{AC} , which substantially determines the speed of the system as a whole, was measured in open loop configuration. That is, the signal fed into pool A with a sweep generator was monitored in pool C with the novel input probe (*a*). In the case of intact axons, the probe shows a pronounced high-pass behaviour associated with the nodal membrane, which was confirmed theoretically by multiplying the transfer functions F_m and F_{DC} (cf. Fig. 8).

The two lower curves (Fig. 5*b* and *c*) were obtained in closed loop configuration, the same signal as in Fig. 5*a* being applied to the command input of the measurement system. Both signals, the error signal (*b*) measured with the novel input probe in pool C as well as the transfer function U_A/U_{com} measured conventionally in pool A (*c*, cf. Fig. 9 above), serve as adjustment criteria for the amplifiers A1 and A2. They are therefore indispensable for guaranteeing constant and hence comparable experimental conditions with optimized quality of control.

The bandwidth (-3 dB) recorded in pool A with the listed improvements was 100 – 300 kHz. Therefore, in order to compensate the disturbing influence of the series resistance electronically (Schumann 1980; Sigworth 1980; Albers et al. 1989; Bethge et al. 1991) the positive feedback loop requires only a 100-kHz low-pass filter which has no measurable effect on the membrane current records.

In contrast, the low zero-drift also essential for constant experimental conditions is achievable with no special technical arrangements: by repeatedly checking the inactivation variable of sodium permeability, h_∞ , it was set to 0.8 in the ordinary way, by correcting a d.c. voltage source connected to the command input (not shown in Fig. 1) of A2. As a result, slow changes in electrode polarization and diffusion potentials are rendered sufficiently ineffective that they cause no zero-drift even in experiments lasting many hours (Bethge et al. 1991; Bohuslavizki et al. 1994).

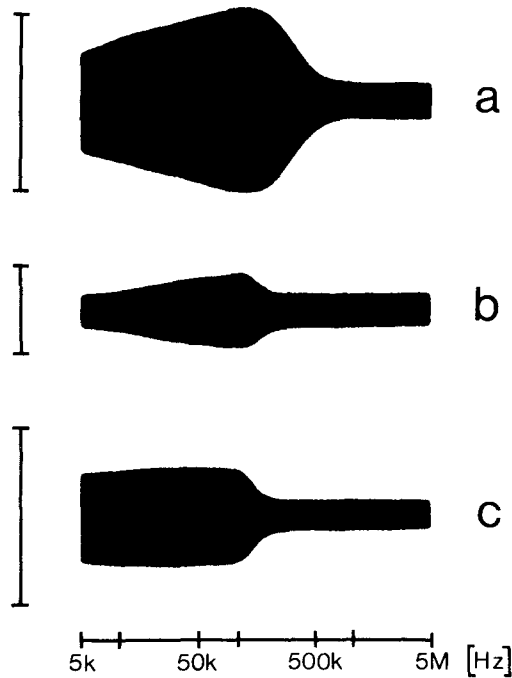


Figure 5. Measured frequency responses of different components of the experimental setup as produced by a sweep generator. *a*: transfer function of feedback components of the potential-controlling loop, including the node under investigation plus corresponding internode \overline{DC} plus input probe. The generator and the recording oscilloscope were connected to pool A and to the output of the input probe, respectively. The resting potential was adjusted to -70 mV by U_A (Fig. 1). Open loop configuration. *b*: transfer function of the error signal of the potential-controlling loop. The generator and the oscilloscope were connected to the command input of the setup and to the output of the input probe, respectively. Closed loop configuration with A1 and A2 adjusted for best performance. Without positive feedback. *c*: transfer function of membrane potential corresponding to the calculated curve of Figure 9 (above). The generator and the oscilloscope were connected to the command input of the setup and pool A, respectively. Closed loop configuration with A1 and A2 adjusted for best performance. Curves *b* and *c* refer to the same command voltage, without positive feedback. Vertical bars denote 10 mV (*a*), 5 mV (*b*) and 100 mV (*c*).

Ramp criterion

When the ramp criterion introduced in this paper was used for compensating the influence of the series resistance, the time constants of sodium inactivation, τ_h , found by fitting curves to current records, were independent of the magnitude of the available sodium current (Fig. 6, triangles). This was not the case in the

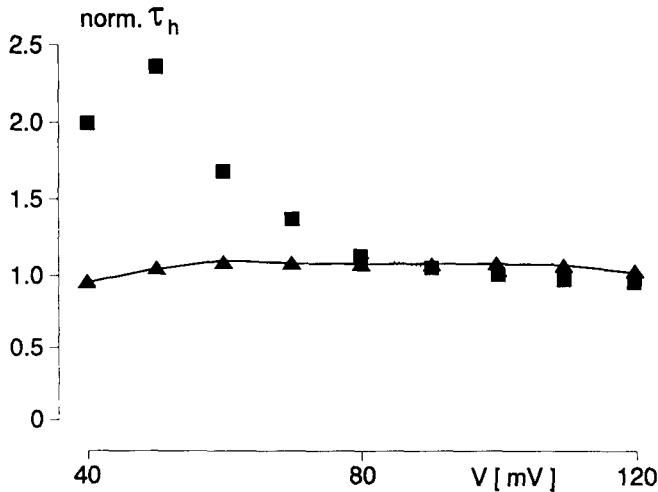


Figure 6. Influence of the series resistance on the time constants of sodium inactivation, τ_h , obtained by curve-fitting with Equation 1. Abscissa: test-pulse amplitude V in mV. Ordinate: normalized time constants, norm. τ_h , determined after prepulses with $V = -40$ mV and duration 50 ms and normalized with respect to τ_h determined after prepulses with $V = +15$ mV and duration 50 ms. Squares: without compensation. Triangles: with compensation applying the ramp criterion. All data from a single axon.

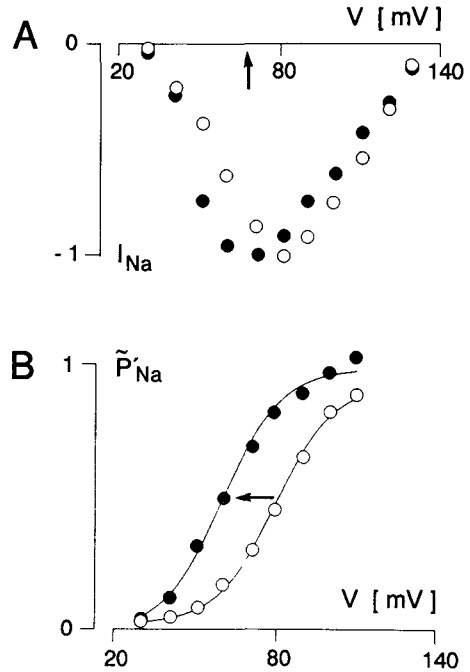
absence of compensation (squares).

To estimate the extent to which the amount of compensation influences the recorded behaviour of the membrane currents, the first step was to obtain the peak sodium current-voltage relations measured with rectangular pulses (Fig. 7A). As is evident in the figure, the symmetry criterion was used for the open symbols. Remarkably, the peak of the curve lies to the right of the membrane potential $E = 0$ mV (arrow), which implies a stronger compensation than when the so-called $E = 0$ criterion is used, in which case the curve peak coincides with $E = 0$ mV by definition. Use of the ramp criterion produces a distinctly asymmetric curve (filled symbols) without appreciably affecting the amplitude of the curve maximum.

For further evaluation the current records from which the peak sodium currents were derived were first converted to permeabilities with the constant-field equation (Dodge and Frankenhaeuser 1959) in the usual way (for details, see Bohuslavizki et al. 1994). Because in this calculation we considered only the potential range between $V = 40$ mV and $V = 110$ mV (cf. Albers et al. 1989), for the subsequent fitting of curves to the individual current records we could use the simplified equation (Frankenhaeuser 1960a).

$$P_{Na} = P'_{Na} \cdot \{1 - \exp(-t/\tau_m)\}^a \cdot \exp(-t/\tau_h) \quad (1)$$

Figure 7. Setting of positive feedback. *A*: current-voltage relations; abscissa: test-pulse amplitude V in mV, arrow: zero membrane potential; ordinate: normalized peak sodium currents, I_{Na} . Two runs on one axon. *B*: median sodium permeabilities \tilde{P}'_{Na} as calculated by the constant-field equation (Dodge and Frankenhaeuser 1959) and by fitting Equation 1 to current records derived from a total of 10 runs on six axons (nonlinear regression coefficient $\tau_{nl} > 0.995$ throughout). Abscissa: test-pulse amplitude V in mV. Ordinate: P'_{Na} normalized to the maxima of the respective continuous curves, \bar{P}_{Na} , which were derived by fitting Equation 2 to the respective P'_{Na} values. Open symbols: application of the symmetry criterion. Filled symbols: application of the ramp criterion.



where τ_m and τ_h are the time constants of activation and inactivation of sodium permeability, respectively, and a is the exponent of the activation system. The potential dependence of P'_{Na} is shown in Fig. 7.

To quantify the differences between the P'_{Na} values obtained with the conventional symmetry criterion (open symbols) and those found when the new ramp criterion is used (filled symbols), the equation

$$P'_{Na} = \bar{P}_{Na} \cdot \left[\frac{1}{1 + \exp[(V_P - V)/k_P]} \right]^a \quad (2)$$

(Benoit and Dubois 1987) was fitted to both series of measurements; here V_P represents the position of each curve on the potential axis, k_P is its maximal slope and a is its exponent. The extrapolated maxima of the calculated curves gave the permeability constant \bar{P}_{Na} for each; it is used to normalize the P'_{Na} values to be compared. It is clear that the slope of the curves, k_P , is unaffected by the difference in compensation criterion. Furthermore, the exponent a in both cases is 1.0, to a close approximation (range: 1.0–1.4). However, the new ramp criterion gives a P'_{Na} curve that is shifted in the negative direction by $V \approx 20$ mV, which implies a smaller amount of positive feedback (cf. Koppenhöfer et al. 1984).

Discussion

Quality of control

The high speed of control in the measuring system described here is achieved primarily by the novel input probe, which differs from all prior measuring systems of this kind for the transfer function of the internode \overline{DC} (Fig. 2) in that it allows the low-pass characteristics introduced by the input and by pool B to be neglected up to several hundred kHz (cf. Albers et al. 1989, Fig. 4). This feature, in combination with the optimized adjustment of the control amplifiers A1 and A2, to the frequency response of individual axons and also of the compensation network CN to the internode \overline{DE} , produces a quality of control not previously attained. This is evident in the frequency response of the control system routinely monitored in pool A (Fig. 5c) and in the error signal likewise routinely monitored in pool C *versus* ground, which exhibits a weak maximum in the region of the system corner frequency measured in pool A and, toward the lower frequencies, becomes so small as to disappear in the noise (not shown). With compensation of the influence of the series resistance, especially the frequency response measured in pool A appears a peak depending on the amount of positive feedback (not shown). Altogether, the reliability of the data that can now be obtained seems to depend merely on peculiarities of the individual preparation (see below).

The permeability curves in Fig. 7 gave the value 1 for the exponent a of sodium activation, which was evidently largely independent of the amount of positive feedback. Therefore they designate the so-called activation curve of sodium permeability and hence are directly comparable with the corresponding curves of Frankenhaeuser (1960a), Koppenhöfer and Schmidt (1968) and Albers and coworkers (1989). Different amounts of positive feedback clearly shift the activation curve. $m_\infty = f(V)$, along the potential axis, thereby changing both m_∞ and the time constant τ_m (Albers et al. 1989); hence the so-called standard data for sodium permeability of the nodal membrane (Frankenhaeuser 1960a) need to be revised in the light of present knowledge, especially with respect to the stringency of reasoning based on these data (Frankenhaeuser and Huxley 1964; Frankenhaeuser 1965).

Curves fit to single current records, unlike the P'_{Na} curves, gave values of the exponent a between 1 and more than 30 (Bohuslavizki et al. 1994). We do not explain this discrepancy by invoking so-called gating currents (Neumcke et al. 1976), but instead ascribe it to the complex electrical access to the nodal membrane (Berthold and Rydmark 1983 a,b), to the rather obscure interactions among the sodium channels, (von der Heydt et al. 1981) and, above all, to the time resolution of such measurements, which now is limited entirely by the preparation itself. It should also be mentioned in this regard that whereas in the past there has often been some controversy over the behaviour of the sodium outward currents,

which has given rise to disputes about the need to replace the concept of conductance with a permeability defined by the constant-field equation (Frankenhaeuser 1960b; Albers et al. 1989), from a present-day standpoint we regard these views as overinterpretations without experimental foundation.

In other words: even the optimized measuring system presented here is evidently not capable of reproducing the onset of sodium activation in current records, so that illusory delays appear that are not discernible in the P'_{Na} curves of Fig. 7 because these are based mostly on data taken from later parts of the current records, which are less subject to error. In any case, we consider the above-mentioned discrepancy as insufficient to call into question the validity of the HHF description for the myelinated axon, since so far every step towards system optimization has proved merely to confirm the validity of that description as originally formulated (Koppenhöfer et al. 1984; Wiese and Koppenhöfer 1988; Albers et al. 1989). The system optimization presented in this paper is so effective that even in the region of the negative branch of the current-voltage curve, where measurements are particularly problematic, the kinetics of sodium inactivation is independent of current strength (cf. Fig. 6). This finding, too, can be taken as further evidence of the precision with which the HHF description applies to the node of Ranvier.

Limitations of the measuring system

The reliability of all membrane current records at the node of Ranvier is undoubtedly still limited by the special features of the axon cylinder plus Schwann cell as a functional unit. Chief among the limitations is the time resolution of the current records, which has often been greatly overestimated. The shadow of doubt this casts on all previous assertions about processes as rapid as capacitive currents, so-called sodium tail currents and gating currents is beyond the scope of the present discussion.

One problem that has rarely been discussed in the literature is the occasional marked variability of current records despite constant experimental conditions. In our opinion it is not justified to ascribe this phenomenon generally to differences in mechanical damage during manipulation of the preparation alone, because there are functionally aberrant axons that exhibit no light-microscopically discernible damage after being dissected and mounted in the recording chamber and, furthermore, have excellent long-term electrical stability with respect to all measurable parameters as long as care is taken to keep $h_{\infty} = 0.8$ and the positive feedback optimal throughout the experiment (cf. Bohuslavizki et al. 1994).

There evidently exist two main types of axons that differ functionally, in typical ways, from so-called normal axons. The one group is characterized by an unduly flat inactivation curve; sometimes it can be impossible to set $h_{\infty} = 0.8$ without destroying the membrane by making the hyperpolarizing voltages in pool A much greater than +100 mV. The second group is characterized by an almost

complete absence of potassium outward currents, with sodium outward currents much larger than average (cf. Frankenhaeuser and Århem 1975). Representatives of both groups are occasionally encountered in remarkably large numbers. In the course of experiments spanning several years we have not been able to correlate these occasions of frequent occurrence with unusual conditions in which the animals were kept, or with any other parameters.

We suggest that such out-of-the-ordinary axons result from as yet unknown, and evidently extremely variable influences of the Schwann cell on the reliability of the membrane current records. This interpretation is supported by the finding that under so-called current clamp conditions, even in the absence of electrotonus, sometimes negative potentials are recorded in pool A, though the action potentials are otherwise unremarkable. Electrode potentials are certainly not responsible for such deviant behaviour. However, care must be taken that the current-carrying electrodes under experimental conditions have polarization resistances of only a few $k\Omega$, because otherwise remarkable features like those described above can be simulated.

Setting of positive feedback

The general category of problems encountered in finding an optimal compensation criterion for the influence of series resistance became clear as soon as the effect of different amounts of compensation on the sodium current-voltage curve was demonstrated (Koppenhöfer et al. 1984). The criteria previously used demanded different amounts of compensation and thus also implied series resistances of different magnitudes. The lowest values are those derived with the ramp criterion; the especially large scatter found here is certainly the result of considerable morphological differences among individual nodal gaps, which in practice can be further emphasized by differences in the amount of mechanical disturbance of the axons during dissection (Koppenhöfer et al. 1987). Our observation that in some axons the series resistance can be effectively zero, however, is in marked contradiction to calculations based on morphometric studies of central axons of the cat, which gave values around 0.5–2 $M\Omega$ for the nodal-gap extracellular space (Berthold and Rydmark 1983a). Either the observed morphological similarity between central axons of the cat and peripheral axons of *Xenopus* (M. Rydmark, personal communication) is more problematic than it seemed after all, or the electrical behaviour of the nodal gap structure contains highly effective, conductivity-increasing mechanisms that are as yet largely unknown.

Among the compensation criteria we have tested so far, the ramp criterion is distinguished by minimizing the number of necessary assumptions, inasmuch as the time constants of the membrane currents depend exclusively on the actual membrane potential. This fundamental aspect of the HHF description was called into question at an early stage (Frankenhaeuser 1963). We regard the findings at

that time which, as it happens, were reproducible (Koppenhöfer 1967) as artefacts of the measurement technique, very much like the earlier statements about the delay of sodium activation (Neumcke et al. 1976).

Further applications of the new input probe

The input probe we have developed is characterized by the following: 1. Very low input capacitance with high input resistance. 2. Low-drift cathode-follower behaviour, from d.c. into the MHz range. 3. Low output impedance, which permits extensive shielding devices to be driven with no reaction. 4. Self-compensating capacitance neutralization and hence, due to the absence of additional phase shifts, no tendency to oscillate, which makes them particularly suitable for feedback systems. 5. Favourable signal-to-noise ratio, therefore particularly suitable for low signal levels.

The probe is thus especially well suited for high-resolution potential measurements with microelectrodes, because with it the faulty compensation typical of the widely used capacitance neutralization according to Bell (1949) cannot occur; this applies in particular to patch-clamp measurements as a result of the specially high source resistance of these preparations, but also to prolonged recordings with skin electrodes and the associated changes in input time constants. The many possible applications in other technical areas will not be detailed here.

Appendix

The measuring system we use (Fig. 2) can be represented as a flow diagram (see Fig. 8) in which F stands for the partial transfer functions of the components identified in the subscripts: A1, A2, A3 (active elements), m (nodal membrane), DC and ED (internodal sections) and CN (external compensation network for linearizing the current-measuring internode ED).

Application of the ordinary rules of calculation (Pressler 1967) gives the transfer function of the command voltage U_{com} :

$$\frac{U_A}{U_{com}} = \frac{-F_{A1} \cdot F_{A2} \cdot F_{DC} \cdot F_{ED} \cdot F_{CN}}{(1 - F_{A1} \cdot F_{DC} \cdot F_m) \cdot (1 - F_{A3} \cdot F_{A2}) - F_{A1} \cdot F_{A2} \cdot F_{DC} \cdot F_{ED} \cdot F_{CN}} \quad (3)$$

In the same way we obtain the transfer function

$$\frac{U_E}{U_m} = \frac{F_{A1} \cdot F_{A2} \cdot F_{DC}}{(1 - F_{A1} \cdot F_{DC} \cdot F_m) \cdot (1 - F_{A2} \cdot F_{A3}) - F_{A1} \cdot F_{A2} \cdot F_{DC} \cdot F_{ED} \cdot F_{CN}}$$

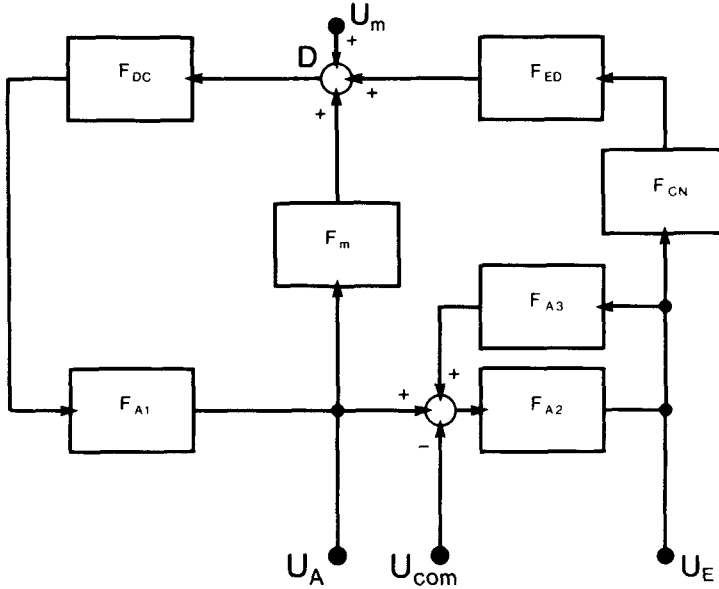


Figure 8. Flow diagram of the measuring system for calculation of the transfer functions U_A/U_{com} and U_E/I_m in the closed-loop configuration. U_A, U_E : voltages in the respective compartments. U_{com} : command voltage. D: point inside the axon close to the node. U_m : potential fed into point D. Open circles: summing points. F_m, F_{DC}, F_{ED} : transfer functions of the nodal membrane and the adjacent internodes. Concerning the remaining subscripts see Fig. 1.

It follows that

$$F_{G1} = -F_{ED} \cdot F_{CN} \cdot F_{G2}.$$

If the transfer function of the currents I_m generated when the membrane potential is changed is defined as

$$F_{G3} = \frac{U_E}{I_m} = \frac{U_E}{U_m} \cdot \frac{1}{G_D}$$

and the conductance G_D (Kneip 1987) is replaced by the radial impedance in pool A, Z_1 , by the intraaxonal longitudinal impedance in pool E, Z_6 , and by the associated transfer functions F_m and F_{ED} , it follows that

$$F_{G3} = F_{G2} \cdot \frac{Z_1 \cdot Z_6}{Z_6 \cdot (F_m^{-1} - 1) + Z_1 \cdot (F_{ED} - 1)}.$$

With

$$\frac{F_m}{F_{ED}} = \frac{Z_6}{Z_1}$$

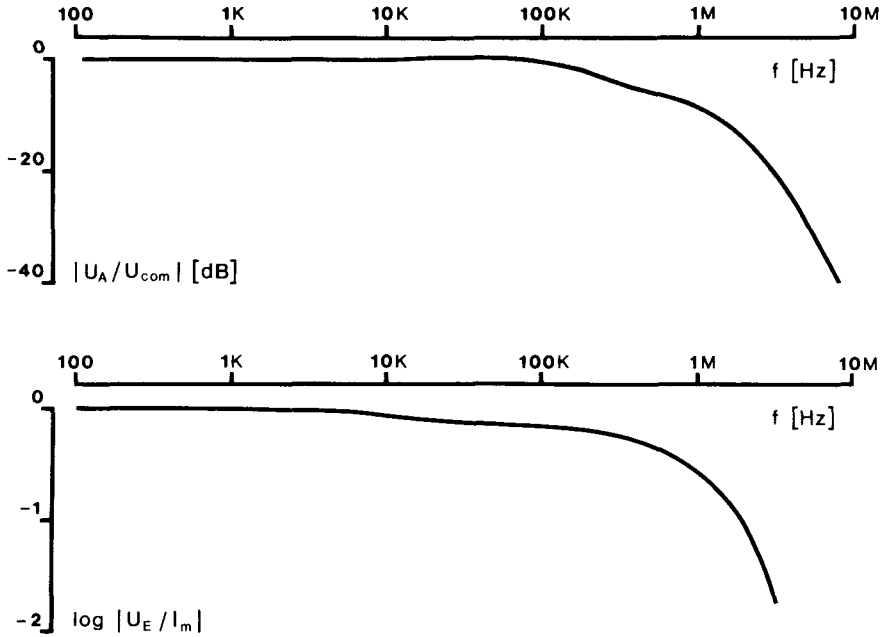


Figure 9. Calculated transfer functions U_A/U_{com} and U_E/I_m of the closed loop configuration for $F_{A3} = 0$, i.e. without positive feedback, and for best performance, i.e. adjustment of A1 and A2 for a phase reserve of $\alpha = 60^\circ$ (Tietze and Schenk 1980) using the standard data given by Stämpfli and Hille (1976). Note that the lower curve was scaled to the d.c. transfer constant.

it follows after rearrangement and simplification that

$$F_{G3} \approx \frac{Z_6}{F_{CN}} \cdot F_{G1}. \tag{4}$$

The numerical solutions of Equations 3 and 4 are shown in Fig. 9. The two curves are similar in shape. That is, the transfer function U_A/U_{com} , easily measurable in practice with a sweep generator, can serve as a reliable measure of the membrane currents, and hence of the time resolution achievable in an individual experiment.

References

Albers M., Bohuslavizki K. H., Koppenhöfer E. (1989): High standard one-loop potential clamp device for Ranvier nodes. *Gen. Physiol. Biophys.* **8**, 409—433
 Bell P. R. (1949): Negative-capacity amplifier. In: *Waveform.* (M.I.T. Rad. Lab. Ser., Vol. 19) (Eds. B. Chance et al.), pp. 767—770, Mc Graw-Hill, New York

- Benoit E., Dubois J.-M. (1987): Properties of maintained sodium current induced by a toxin from *Androctonus* scorpion in frog node of Ranvier. *J. Physiol. (London)* **383**, 93—114
- Berthold C.-H., Rydmark M. (1983a): VI. Anatomy of the paranode-node-paranode region in the cat. *Experientia* **39**, 964—976
- Berthold C.-H., Rydmark M. (1983b): Electron microscopic serial section analysis of nodes of Ranvier in lumbosacral spinal roots of the cat: ultrastructural organization of nodal compartments in fibres of different sizes. *J. Neurocytol.* **12**, 475—505
- Bethge E. W., Bohuslavizki K. H., Hänsel W., Kneip A., Koppenhöfer E. (1991): Effect of some potassium channel blockers on the ionic currents in myelinated nerve. *Gen. Physiol. Biophys.* **10**, 225—244
- Binstock L., Adelman Jr. W. J., Senft J. P., Lecar H. (1975): Determination of the resistance in series with the membranes of giant axons. *J. Membrane Biol.* **21**, 25—47
- Bohuslavizki K. H., Hänsel W., Kneip A., Koppenhöfer E., Niemöller E., Sanmann K. (1994): Mode of action of psoralens, benzofurans, acridinons and coumarins on the ionic currents in myelinated nerve fibres and its significance in demyelinating diseases. *Gen. Physiol. Biophys.*, **13**, 309—328
- Chiu S. Y. (1980): Asymmetry currents in the mammalian myelinated nerve. *J. Physiol. (London)* **209**, 499—519
- Dodge F. A., Frankenhaeuser B. (1958): Membrane currents in isolated frog nerve fibre under voltage clamp conditions. *J. Physiol. (London)* **143**, 76—90
- Dodge F. A., Frankenhaeuser B. (1959): Sodium currents in the myelinated nerve fibre of *Xenopus laevis* investigated with the voltage clamp technique. *J. Physiol. (London)* **148**, 188—200
- Frankenhaeuser B. (1957): A method for recording resting and action potentials in the isolated myelinated nerve fibre of the frog. *J. Physiol. (London)* **135**, 550—559
- Frankenhaeuser B. (1960a): Quantitative description of sodium currents in myelinated nerve fibres of *Xenopus laevis*. *J. Physiol. (London)* **151**, 491—501
- Frankenhaeuser B. (1960b): Sodium permeability in toad nerve and in squid nerve. *J. Physiol. (London)* **152**, 159—166
- Frankenhaeuser B. (1963): Inactivation of the sodium-carrying mechanism in myelinated nerve fibres of *Xenopus laevis*. *J. Physiol. (London)* **169**, 445—451
- Frankenhaeuser B. (1965): Computed action potential in nerve from *Xenopus laevis*. *J. Physiol. (London)* **180**, 780—787
- Frankenhaeuser B., Århem P. (1975): Steady state current rectification in potential clamped nodes of Ranvier (*Xenopus laevis*). *Phil. Trans. Roy. Soc. London B.* **270**, 515—525
- Frankenhaeuser B., Huxley A. F. (1964): The action potential in the myelinated nerve fibre of *Xenopus laevis* as computed on the basis of voltage clamp data. *J. Physiol. (London)* **171**, 302—315
- Hodgkin A. L., Huxley A. F. (1952): A quantitative description of membrane current and its application to conduction and excitation in nerve. *J. Physiol. (London)* **117**, 500—544
- Hodgkin A. L., Huxley A. F., Katz B. (1949): Ionic currents underlying activity in the giant axon of the squid. *Arch. Sci. Physiol.* **3**, 129—150
- Hodgkin A. L., Huxley A. F., Katz B. (1952): Measurement of current-voltage relations in the membrane of the giant axon of *Loligo*. *J. Physiol. (London)* **116**, 424—448

- Kneip A (1987) Ionenstrommessungen an myelinisierten Nervenfasern unter optimierten Meßbedingungen Das Verfahren nach Frankenhaeuser Thesis, University of Kiel
- Kootsey J M, Johnson E A (1973) Buffer amplifier with femtofarad input capacity using operational amplifiers IEEE Trans Biomed Eng **20**, 389—391
- Koppenhofer E (1967) Die Wirkung von Tetraethylammoniumchlorid auf die Membranstrome Ranvierscher Schnurringe von *Xenopus laevis* Pflugers Arch **293**, 34—55
- Koppenhofer E, Bohuslavizki K H (1988) Inconsistent sodium current records derived on Ranvier nodes with a commercially available potential clamp device according to Nonner Gen Physiol Biophys **7**, 557—567
- Koppenhofer E, Schmidt H (1968) Die Wirkung von Skorpiongift auf die Ionenströme des Ranvierschen Schnurrings I Die Permeabilitäten P_{Na} und P_K Pflugers Arch **303**, 133—149
- Koppenhofer E, Schumann H (1979) Sodium currents in the node of Ranvier with compensation of the effect of the series resistance Pflugers Arch **382**, R 37
- Koppenhofer E, Schumann H (1981) A method for increasing the frequency response of voltage clamped myelinated nerve fibres Pflugers Arch **390**, 288—289
- Koppenhofer E, Wiese H, Schumann H, Wittig J (1984) Experimente zum Einfluß des Serienwiderstandes auf die Potentialabhängigkeit der Natriumspitzenströme des Ranvierschen Schnurrings Funkt Biol Med **3**, 61—64
- Koppenhofer E, Sommer R -G, Froese U (1987) Effects of benzocaine and its isomers on sodium permeability and steady state sodium inactivation in the myelinated nerve obtained by an improved dissection technique Gen Physiol Biophys **6**, 209—222
- Koppenhofer E, Sommer R -G, Bohuslavizki K H (1992) Die Erforschung der Funktion peripherer Nerven Eine Bestandsaufnahme TW Neurologie Psychiatrie **6**, 25—39
- Kuhn Th S (1961) The function of measurement in modern physical science Isis **52**, 161—193
- Marmont G (1949) Studies on the axon membrane I A new method J Cell Comp Physiol **34**, 351—382
- Moore J W, Hines M, Harris E M (1984) Compensation for resistance in series with excitable membranes Biophys J **46**, 507—514
- Mozhayev G A (1968) The cathode follower with small input capacity for cytophysiological aims Tsitologiya **10**, 148—150
- Mozhayeva G N, Naumov A P, Negulyaev Yu A, Nosyreva E D (1977) The permeability of aconitine-modified sodium channels to univalent cations in myelinated nerve Biochim Biophys Acta **466**, 461—473
- Neher E (1974) Elektronische Meßtechnik in der Physiologie Springer, Berlin
- Neumcke B, Nonner W, Stampfl R (1976) Asymmetrical displacement current and its relation with the activation of sodium current in the membrane of frog myelinated nerve Pflugers Arch **363**, 193—203
- Nonner W (1969) A new voltage clamp method for Ranvier nodes Pflugers Arch **309**, 176—192
- Pressler G (1967) Regelungstechnik Bibliographisches Institut, Mannheim
- Purves R D (1981) Microelectrode Methods for Intracellular Recording and Ionophoresis Academic Press, London
- Ramon F, Anderson N, Joyner W, Moore J W (1975) Axon voltage clamp simulations IV A multicellular preparation Biophys J **15**, 55—69

- Schumann H. (1980): Kompensation der elektrischen Auswirkungen des perinodalen Zugriffswiderstandes bei Ionenstrommessungen am Ranvierschen Schnürring. Thesis, University of Kiel
- Schumann H., Koppenhöfer E., Wiese H. (1983): Compensation of the low-pass filter properties of the current measuring internode in potential-clamped myelinated nerve fibres. *Gen. Physiol. Biophys.* **2**, 287—295
- Sigworth F. J. (1980): The variance of sodium current fluctuations at the node of Ranvier. *J. Physiol. (London)* **307**, 97—129
- Smith Jr. Th. G., Lecar H., Redman St. J., Gage P. W. (1985): Voltage and Patch Clamping with Microelectrodes. Amer. Physiol. Soc., Bethesda
- Sommer R.-G., Schumann H., Koppenhöfer E. (1982): Changes in myelinated nerve fibres caused by insulating layers. *Acta Physiol. Scand.* **114**, 413—417
- Stämpfli R., Hille B. (1976): 1. Electrophysiology of the peripheral myelinated nerve. In: *Frog Neurobiology*. (Eds. R. Llinàs, W. Precht), pp. 3—32, Springer, Berlin
- Tietze U., Schenk C. (1980): Halbleiterschaltungstechnik. Springer, Berlin
- von der Heydt I., von der Heydt N., Obermayr G. M. (1981): Statistical model of current-coupled ion channels in nerve membrane. *Z. Phys. B – condensed matter* **41**, 153—164
- Wiese H., Duchâteau R. (1984): Measurement of absolute membrane potential with the potential clamp system of Nonner. *Gen. Physiol. Biophys.* **3**, 511—512
- Wiese H., Koppenhöfer E. (1988): Minimizing the influence of the series resistance in potential clamped Ranvier nodes. *Gen. Physiol. Biophys.* **7**, 143—156

Final version accepted October 15, 1994